

# Intrinsic functional connectivity differentiates minimally conscious from unresponsive patients

Athena Demertzi,<sup>1,\*</sup> Georgios Antonopoulos,<sup>1,\*</sup> Lizette Heine,<sup>1</sup> Henning U. Voss,<sup>2</sup> Julia Sophia Crone,<sup>3,4,5</sup> Carlo de Los Angeles,<sup>6</sup> Mohamed Ali Bahri,<sup>7</sup> Carol Di Perri,<sup>1</sup> Audrey Vanhauzenhuyse,<sup>8</sup> Vanessa Charland-Verville,<sup>1</sup> Martin Kronbichler,<sup>3,4</sup> Eugen Trinka,<sup>5</sup> Christophe Phillips,<sup>7</sup> Francisco Gomez,<sup>9</sup> Luaba Tshibanda,<sup>10</sup> Andrea Soddu,<sup>11</sup> Nicholas D. Schiff,<sup>12,13</sup> Susan Whitfield-Gabrieli<sup>6,\*</sup> and Steven Laureys<sup>1,\*</sup>

\*These authors contributed equally to this work.

Despite advances in resting state functional magnetic resonance imaging investigations, clinicians remain with the challenge of how to implement this paradigm on an individualized basis. Here, we assessed the clinical relevance of resting state functional magnetic resonance imaging acquisitions in patients with disorders of consciousness by means of a systems-level approach. Three clinical centres collected data from 73 patients in minimally conscious state, vegetative state/unresponsive wakefulness syndrome and coma. The main analysis was performed on the data set coming from one centre (Liège) including 51 patients (26 minimally conscious state, 19 vegetative state/unresponsive wakefulness syndrome, six coma; 15 females; mean age  $49 \pm 18$  years, range 11–87; 16 traumatic, 32 non-traumatic of which 13 anoxic, three mixed; 35 patients assessed > 1 month post-insult) for whom the clinical diagnosis with the Coma Recovery Scale-Revised was congruent with positron emission tomography scanning. Group-level functional connectivity was investigated for the default mode, frontoparietal, salience, auditory, sensorimotor and visual networks using a multiple-seed correlation approach. Between-group inferential statistics and machine learning were used to identify each network's capacity to discriminate between patients in minimally conscious state and vegetative state/unresponsive wakefulness syndrome. Data collected from 22 patients scanned in two other centres (Salzburg: 10 minimally conscious state, five vegetative state/unresponsive wakefulness syndrome; New York: five minimally conscious state, one vegetative state/unresponsive wakefulness syndrome, one emerged from minimally conscious state) were used to validate the classification with the selected features. Coma Recovery Scale-Revised total scores correlated with key regions of each network reflecting their involvement in consciousness-related processes. All networks had a high discriminative capacity (>80%) for separating patients in a minimally conscious state and vegetative state/unresponsive wakefulness syndrome. Among them, the auditory network was ranked the most highly. The regions of the auditory network which were more functionally connected in patients in minimally conscious state compared to vegetative state/unresponsive wakefulness syndrome encompassed bilateral auditory and visual cortices. Connectivity values in these three regions discriminated congruently 20 of 22 independently assessed patients. Our findings point to the significance of preserved abilities for multisensory integration and top-down processing in minimal consciousness seemingly supported by auditory-visual crossmodal connectivity, and promote the clinical utility of the resting paradigm for single-patient diagnostics.

- 1 Coma Science Group, GIGA-Research & Cyclotron Research Centre, University and CHU University Hospital of Liège, Liège, Belgium
- 2 Department of Radiology and Citigroup Biomedical Imaging Centre, Weill Cornell Medical College, New York, USA
- 3 Department of Psychology and Centre for Neurocognitive Research, Salzburg, Austria

- 4 Neuroscience Institute and Centre for Neurocognitive Research, Christian-Doppler-Klinik, Paracelsus Private Medical University, Salzburg, Austria
- 5 Department of Neurology, Christian-Doppler-Klinik, Paracelsus Private Medical University, Salzburg, Austria
- 6 Martinos Imaging Centre at McGovern Institute for Brain Research, Massachusetts Institute of Technology, Cambridge MA, USA
- 7 Cyclotron Research Centre, University of Liège, Liège, Belgium
- 8 Department of Algology and Palliative Care, CHU University Hospital of Liège, Liège, Belgium
- 9 Computer Science Department, Universidad Central de Colombia, Bogota, Colombia
- 10 Department of Radiology, CHU University Hospital of Liège, Liège, Belgium
- 11 Brain and Mind Institute, Department of Physics and Astronomy, Western University, London, Ontario, Canada
- 12 Department of Neuroscience, Weill Cornell Graduate School of Medical Sciences, New York, USA
- 13 Department of Neurology and Neuroscience, Weill Cornell Medical College, New York, USA

Correspondence to: Demertzi Athena,  
Coma Science Group, Cyclotron Research Centre,  
Allée du 6 août n° 8, Sart Tilman B30,  
Université de Liège, 4000 Liège, Belgium.  
E-mail: a.demertzi@ulg.ac.be

**Keywords:** consciousness; traumatic brain injury; resting state connectivity; sensory systems; anoxia

**Abbreviations:** CRS-R = Coma Recovery Scale-Revised; MCS = minimally conscious state; UWS = unresponsive wakefulness syndrome; VS = vegetative state

## Introduction

As patients with acute or chronic disorders of consciousness are by definition unable to communicate, their diagnosis is particularly challenging. Patients in coma, for example, lay with eyes closed and do not respond to any external stimulation. When they open their eyes but remain unresponsive to external stimuli they are considered to be in a vegetative state (VS; Jennett and Plum, 1972) or, as most recently coined, unresponsive wakefulness syndrome (UWS; Laureys *et al.*, 2010). When patients exhibit signs of fluctuating yet reproducible remnants of non-reflex behaviour, they are considered to be in a minimally conscious state (MCS; Giacino *et al.*, 2002). To date, the diagnostic assessment of patients with disorders of consciousness is mainly based on the observation of motor and oro-motor behaviours at the bedside (Giacino *et al.*, 2014). The evaluation of non-reflex behaviour, however, is not straightforward as patients can fluctuate in terms of vigilance, may suffer from cognitive (e.g. aphasia, apraxia) and/or sensory impairments (e.g. blindness, deafness), from small or easily exhausted motor activity and pain. In these cases, absence of responsiveness does not necessarily correspond to absence of awareness (Sanders *et al.*, 2012). Alternatively, motor-independent technologies can aid the clinical differentiation between the two patient groups (Bruno *et al.*, 2010).

Up to now, accurate single-patient categorization in MCS and VS/UWS has been performed by means of transcranial magnetic stimulation in combination with EEG (Rosanova *et al.*, 2012; Casali *et al.*, 2013) and by combining different EEG measures (Sitt *et al.*, 2014). In terms of patient separation by means of functional MRI, activation (which utilise sensory stimulation; Schiff *et al.*, 2005; Coleman *et al.*, 2007; Di *et al.*, 2007) and active paradigms (which probe

mental command following; Owen *et al.*, 2006; Monti *et al.*, 2010; Bardin *et al.*, 2012) have been used to detect covert awareness in these patients. An apparent limitation of the latter approaches is that patients may demonstrate motor and language deficits which incommode these assessments and heighten the risk of false-negative findings (Giacino *et al.*, 2014). The application of these paradigms can also be constrained due to each institution's technical facilities.

Alternatively, functional MRI acquisitions during resting state do not require sophisticated setup and surpass the need for subjects' active participation. Past resting state functional MRI-based assessment of patients has focused on the default mode network, which mainly encompasses anterior and posterior midline regions, and which has been involved in conscious and self-related cognitive processes (Raichle *et al.*, 2001; Buckner *et al.*, 2008). Such investigations have shown that default mode network functional connectivity decreases alongside the spectrum of consciousness, moving from healthy controls to patients in MCS, VS/UWS and coma (Boly *et al.*, 2009; Vanhaudenhuyse *et al.*, 2010; Norton *et al.*, 2012; Soddu *et al.*, 2012; Demertzi *et al.*, 2014; Huang *et al.*, 2014). In patients, the precuneus and posterior cingulate cortex of the default mode network have been also characterized by decreases in functional MRI resting state low frequency fluctuations and regional voxel homogeneity (which refers to the similarity of local brain activity across a region) (Tsai *et al.*, 2014). Reduced functional MRI functional connectivity has been further identified for interhemispheric homologous regions belonging to the extrinsic or task-positive network (implicated in the awareness of the environment; Vanhaudenhuyse *et al.*, 2011) in patients as compared to controls (Ovadia-Caro *et al.*, 2012). Reduced interhemispheric connectivity has

been also indicated by means of partial correlations (Maki-Marttunen *et al.*, 2013). In terms of graph theory metrics, comatose patients were shown to preserve global network properties but cortical regions, which worked as hubs in healthy controls, became non-hubs in comatose brains and vice versa (Achard *et al.*, 2011, 2012). Similarly, chronic patients showed altered network properties in medial parietal and frontal regions as well as in the thalamus, and most of the affected regions in unresponsive patients belonged to the so-called ‘rich-club’ of highly interconnected central nodes (Crone *et al.*, 2014). More recently, functional MRI-based single-patient classification has been performed by considering as discriminating feature the neuronal properties of various intrinsic connectivity networks (Demertzi *et al.*, 2014). The discrimination between ‘neuronal’ and ‘non-neuronal’ was based on the spatial and temporal properties (fingerprints) of the identified networks that were extracted by means of independent component analysis (De Martino *et al.*, 2007). According to specific criteria (Kelly *et al.*, 2010), ‘non-neuronal’ components were those that showed activation/deactivation in peripheral brain areas, in the cerebrospinal fluid (CSF) and white matter, as well as those showing high frequency fluctuations ( $>0.1$  Hz), spikes, presence of a sawtooth pattern and presence of thresholded voxels in the superior sagittal sinus. Conversely, ‘neuronal’ were those networks when at least 10% of the activations/deactivations were found in small to larger grey matter clusters localized to small regions of the brain. Based on this definition of neuronality, the ‘neuronal’ properties of the default mode and auditory network were able to separate single-patients from healthy controls with 85.3% accuracy. Nevertheless, the discrimination accuracy between patients in MCS and VS/UWS reached only a chance level (Demertzi *et al.*, 2014).

Taken together, these studies show that the so far resting state functional MRI-based differentiation of patients has been performed either at the group-level or concerned the classification between healthy and pathological groups. As a consequence, clinicians remain with the challenge of how to implement the resting state functional MRI paradigm on an individualized basis for the more challenging discrimination between the MCS and VS/UWS (Edlow *et al.*, 2013). Here, we aimed at promoting the MCS-VS/UWS single-patient differentiation by using resting state functional MRI measurements in this clinical population. To this end, we studied systems-level resting state functional MRI functional connectivity in traumatic and non-traumatic patients with acute and chronic disorders of consciousness with the aim to (i) estimate the contribution of each network to the level of consciousness as determined by behavioural assessment; (ii) rank the capacity of each network to differentiate between patients in MCS and VS/UWS; and (iii) automatically classify independently assessed patients.

## Materials and methods

### Subjects

Three data sets were used, including patients scanned in Liège [to address study aims (i) and (ii)], Salzburg and New York [to address study aim (iii)]. Inclusion criteria were patients in MCS, VS/UWS and coma following severe brain damage studied at least 2 days after the acute brain insult. Patients were excluded when there was contraindication for MRI (e.g. presence of ferromagnetic aneurysm clips, pacemakers), MRI acquisition under sedation or anaesthesia, and uncertain clinical diagnosis. Healthy volunteers were free of psychiatric or neurological history. The study was approved by the Ethics Committee of the Medical School of the University of Liège, the Ethics Committee of Salzburg, and the Institutional Review Board at Weill Cornell Medical College. Informed consent to participate in the study was obtained from the healthy subjects and from the legal surrogates of the patients.

### Data acquisition

All data were acquired on 3 T Siemens TIM Trio MRI scanners (Siemens Medical Solutions). For the Liège data set, 300 multislice  $T_2^*$ -weighted images were acquired with a gradient-echo echo-planar imaging sequence using axial slice orientation and covering the whole brain (32 slices; voxel size =  $3 \times 3 \times 3$  mm<sup>3</sup>; matrix size =  $64 \times 64$ ; repetition time = 2000 ms; echo time = 30 ms; flip angle =  $78^\circ$ ; field of view =  $192 \times 192$  mm). For the Salzburg data set, 250  $T_2^*$ -weighted images (36 slices with 3-mm thickness; repetition time = 2250 ms; echo time = 30 ms; flip angle =  $70^\circ$ ; field of view =  $192 \times 192$  mm). For the New York data set, 180  $T_2^*$ -weighted images were acquired (32 slices; voxel size =  $3.75 \times 3.75 \times 4$  mm<sup>3</sup>; matrix size =  $64 \times 64$ ; repetition time = 2000 ms; echo time = 30 ms; flip angle =  $90^\circ$ ; field of view =  $240 \times 240$  mm).

### Subject-level connectivity analysis

Data analysis is illustrated in Fig. 1.

#### Data preprocessing

Preprocessing and connectivity analyses were performed in the same way for all subjects across the three data sets. The three initial volumes were discarded to avoid  $T_1$  saturation effects. For anatomical reference, a high-resolution  $T_1$ -weighted image was acquired for each subject ( $T_1$ -weighted 3D magnetization-prepared rapid gradient echo sequence). Data preprocessing was performed using Statistical Parametric Mapping 8 (SPM8; [www.fil.ion.ucl.ac.uk/spm](http://www.fil.ion.ucl.ac.uk/spm)). Preprocessing steps included slice-time correction, realignment, segmentation of structural data, normalization into standard stereotactic Montreal Neurological Institute (MNI) space and spatial smoothing using a Gaussian kernel of 6 mm full-width at half-maximum. As functional connectivity is influenced by head motion in the scanner (Van Dijk *et al.*, 2012), we accounted for motion artifact detection and rejection using the artifact detection tool (ART; [http://www.nitrc.org/projects/artifact\\_detect](http://www.nitrc.org/projects/artifact_detect)). Specifically, an image was defined as an outlier (artifact) image if the head displacement in  $x$ ,  $y$ , or

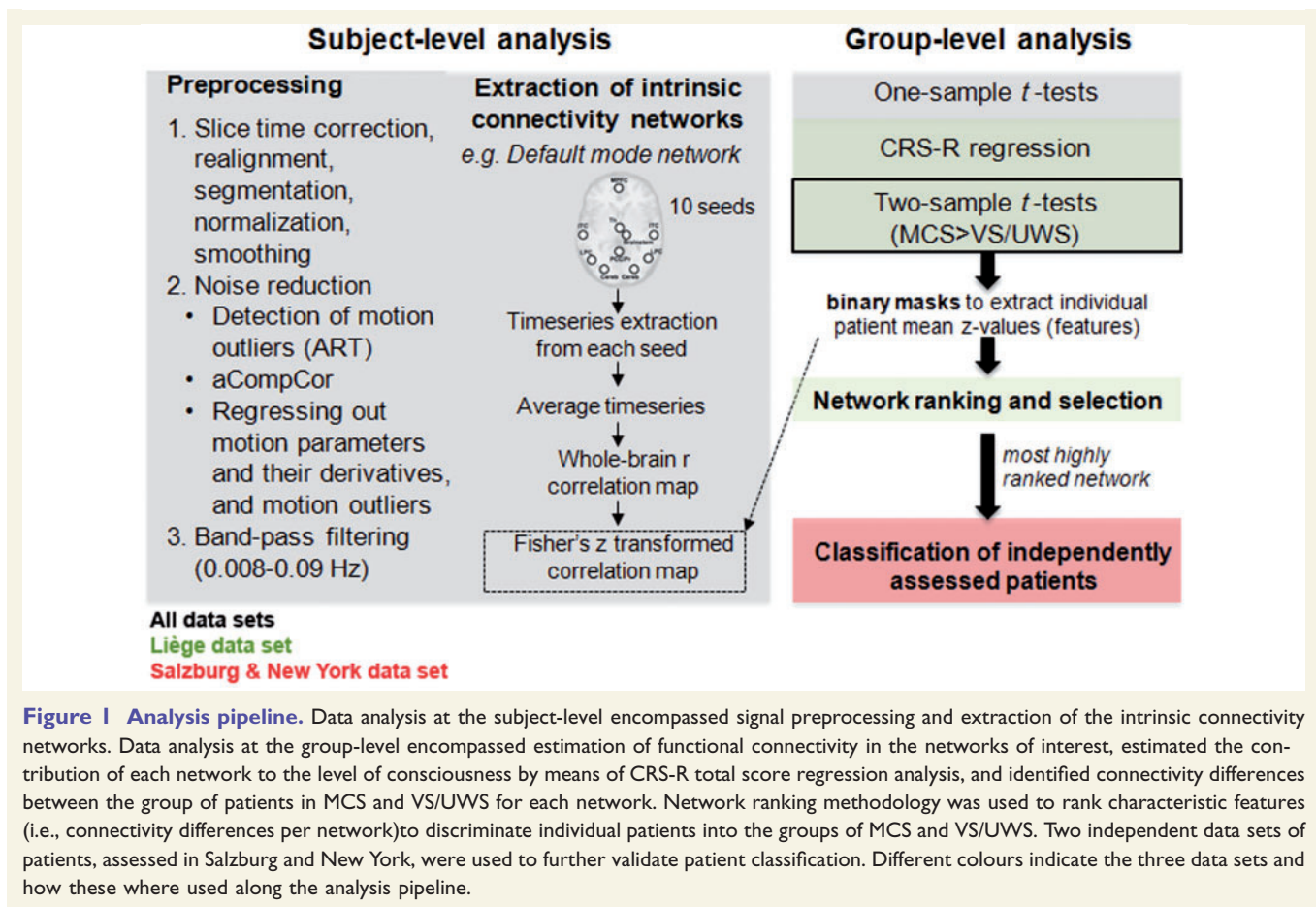


**Figure 1 Analysis pipeline.** Data analysis at the subject-level encompassed signal preprocessing and extraction of the intrinsic connectivity networks. Data analysis at the group-level encompassed estimation of functional connectivity in the networks of interest, estimated the contribution of each network to the level of consciousness by means of CRS-R total score regression analysis, and identified connectivity differences between the group of patients in MCS and VS/UWS for each network. Network ranking methodology was used to rank characteristic features (i.e., connectivity differences per network) to discriminate individual patients into the groups of MCS and VS/UWS. Two independent data sets of patients, assessed in Salzburg and New York, were used to further validate patient classification. Different colours indicate the three data sets and how these were used along the analysis pipeline.

$z$  direction was  $>2$  mm from previous frame, or if the rotational displacement was  $>0.02$  radians from the previous frame, or if the global mean intensity in the image was  $>3$  standard deviations (SD) from the mean image intensity for the entire resting scan. Outliers in the global mean signal intensity and motion were subsequently included as nuisance regressors (i.e. one regressor per outlier within the first-level general linear model). Therefore, the temporal structure of the data was not disrupted.

For noise reduction, previous methods subtracted the global signal across the brain (a controversial issue in resting state analyses; Murphy *et al.*, 2009; Saad *et al.*, 2012; Wong *et al.*, 2012), and the mean signals from noise regions of interest (Greicius *et al.*, 2003; Fox *et al.*, 2005). Here, we used the anatomical component-based noise correction method (aCompCor; Behzadi *et al.*, 2007) as implemented in CONN functional connectivity toolbox (<http://www.nitrc.org/projects/conn/>; Whitfield-Gabrieli and Nieto-Castanon, 2012). The aCompCor models the influence of noise as a voxel-specific linear combination of multiple empirically estimated noise sources by deriving principal components from noise regions of interest and by including them as nuisance parameters within the general linear models. Specifically, the anatomical image for each participant was segmented into white matter, grey matter, and CSF masks using SPM8. To minimize partial voluming with grey matter, the white matter and CSF masks were eroded by one voxel, which resulted in substantially smaller masks than the original segmentations (Chai *et al.*, 2012). The eroded white matter and CSF masks were then

used as noise regions of interest. Signals from the white matter and CSF noise regions of interest were extracted from the unsmoothed functional volumes to avoid additional risk of contaminating white matter and CSF signals with grey matter signals. A temporal band-pass filter of 0.008–0.09 Hz was applied on the time series to restrict the analysis to low frequency fluctuations, which characterize functional MRI blood oxygenation level-dependent resting state activity as classically performed in seed-correlation analysis (Greicius *et al.*, 2003; Fox *et al.*, 2005). Residual head motion parameters (three rotation and three translation parameters, plus another six parameters representing their first-order temporal derivatives) were regressed out.

### Extraction of intrinsic connectivity networks

Functional connectivity adopted a seed-based correlation approach. Seed-correlation analysis uses extracted blood oxygenation level-dependent time series from a region of interest (the seed) and determines the temporal correlation between this signal and the time series from all other brain voxels. Evidently, the selection of the seed region is critical because, in principle, it can lead to as many overlapping networks as the number of possible selected seeds (Cole *et al.*, 2010). Additionally, a network disruption can be expected due to patients' underlying neuropathology, as the chosen seed may no longer be included in the overall network. Using more seed regions, this issue can be overcome and therefore ensure proper network characterization in patients. Here, the seeds

that were selected to replicate the networks were defined as 10-mm (for cortical areas) and 4-mm radius spheres (for subcortical structures) around peak coordinates taken from the literature (Supplementary material). For each network, time series from the voxels contained in each seed region were extracted and then averaged together. In that way, the resulting averaged time course was estimated by taking into account the time courses of more than one regions. The averaged time series were used to estimate whole-brain correlation  $r$  maps that were then converted to normally distributed Fisher's  $z$  transformed correlation maps to allow for group-level comparisons.

## Group-level connectivity analysis

For the Liège data set, one-sample  $t$ -tests were ordered to estimate network-level functional connectivity for patients in MCS, VS/UWS and in coma; the data from healthy controls were used as a reference to ensure proper network characterization. An exploratory analysis looked for network-level connectivity changes as a function of patients' aetiology and chronicity. Two  $2 \times 2$  factorial designs between aetiology (traumatic, non-traumatic)/ chronicity (acute, chronic) and the clinical entities (MCS, VS/UWS) were ordered. If an interaction effect was identified, these variables had to be entered as regressors in the general linear models.

To address the first aim of the study, i.e. to estimate the contribution of each network to the level of consciousness, patients' Coma Recovery Scale-Revised (CRS-R) total scores were used as regressors to determine the relationship between each network's functional connectivity and the level of consciousness. As a control, CRS-R total scores were used as regressors of functional connectivity for the cerebellum network (three regions of interest, Supplementary material), which is known to be minimally implicated in consciousness-related processes (Tononi, 2008; Yu *et al.*, 2015).

To address the second aim of the study, i.e. to determine the capacity of each network to differentiate between patients in MCS and VS/UWS, initially two-sample  $t$ -tests were ordered to identify the regions of each network showing higher functional connectivity in patients in MCS compared to VS/UWS (Liège data set). The resulting difference maps were saved as masks, which were used subsequently for the network ranking and selection step. All results were considered significant  $P < 0.05$  corrected for multiple comparisons at false discovery rate (FWE; cluster-level).

## Network ranking and selection

Using the REX Toolbox (<http://www.nitrc.org/projects/rex/>), the difference masks which were calculated in the previous step were used to extract mean connectivity values (average  $z$ -values across the whole mask) from the first-level contrast images estimated for each network. Therefore, one value per subject per network was created leading to a  $6 \times 1$  vector per subject (i.e.  $45 \times 6$  matrix). These vector values were considered as features in a feature ranking methodology (Saeys *et al.*, 2007) as implemented in Matlab (<http://www.mathworks.nl/help/bioinfo/ref/rankfeatures.html>). The results of the feature (i.e. network) ranking were verified by means of single-feature linear support vector machine classifier (Burges, 1998). Supplementary material contains further details on the network ranking procedure and results.

To address the third aim of the study, i.e. to automatically classify independently assessed patients coming from two other clinical centres, we focused on the network which was ranked most highly during the network ranking procedure. For that network, a linear kernel support vector machine classifier (Burges, 1998) with regularization parameter  $C = 1$  was used. This parameter was chosen based on its wide use in the machine learning procedure (Phillips *et al.*, 2011). The features that were used for the training were individual mean connectivity values extracted from the first-level contrast images using the relevant network binary mask as described above. To avoid single feature classification, hence running the risk of overfitting, more features were included for the classifier's training. The number of features was based on the number of clusters showing higher connectivity in patients in MCS compared to VS/UWS as indicated by the contrast manager of the CONN toolbox during the connectivity analysis (FWE  $P < 0.05$ , cluster-level correction).

## Classification of independently assessed patients

The final validation of the classifier was performed on a new set of connectivity values extracted from independently assessed patients in Salzburg ( $n = 15$ ) and New York ( $n = 7$ ). The data preprocessing, extraction of intrinsic connectivity network, and feature extraction followed an identical procedure as described above for the Liège data set. To test for robustness, we also evaluated whether the same classifier generalized to healthy controls subjects scanned in two centres (Liège, Salzburg; no healthy control data were available for the New York centre).

## Results

### Subjects

In Liège, between April 2008 and December 2012, 177 patients with disorders of consciousness underwent MRI scanning. Of these, 80 (45%) were excluded due to sedation or anaesthesia during scanning. Of the remaining 97 patients scanned in an awake state, five due to change of diagnosis within a week after scanning, 14 because they showed functional communication, 15 due to technical reasons or movement artifacts, and 12 due to incongruence between clinical diagnosis and fluorodeoxyglucose (FDG)-PET scanning (Stender *et al.*, 2014). As regards the latter criterion, we decided to exclude patients showing widespread PET activation in midline and frontoparietal regions while the bedside diagnosis indicated the VS/UWS, in order to avoid confounds due to clinical ambiguity.

The included 51 patients were behaviourally diagnosed with the CRS-R (Giacino *et al.*, 2004) as in MCS = 26, VS/UWS = 19 and coma = 6 (15 females; mean age  $49 \pm 18$  years, range 11–87; 16 traumatic, 32 non-traumatic of which 13 were anoxic, three mixed; 35 patients were assessed in the chronic setting, i.e.  $> 1$  month post-insult). Data from an age-matched group of 21 healthy volunteers

(eight females; mean age  $45 \pm 17$  years; range 19–72) were used as a reference to the connectivity analyses and to validate the generalizability of the classifier without being included in the training. The data set from Salzburg included 10 MCS and five VS/UWS patients; the data set from New York included five MCS, one VS/UWS and one patient emerged from MCS. All patients' demographic and clinical characteristics are summarized in the Supplementary material.

For the Liège data set, the effects of the denoising procedure are summarized in the Supplementary material. Also, the number of motion outlier images did not differ among healthy controls (mean =  $9 \pm 8$ ), patients in MCS (mean =  $22 \pm 17$ ), VS/UWS (mean =  $17 \pm 12$ ), coma (mean =  $2 \pm 2$ ) (for all *t*-tests,  $P < 0.05$ ). The exploratory analysis indicated a main effect for the clinical entity (i.e. MCS, VS/UWS) on the functional connectivity of each network. No interaction was identified between the clinical entity and aetiology (traumatic: MCS = 13, VS/UWS = 1; non-traumatic: MCS = 12 + 1 mixed; VS/UWS = 16 + 2 mixed) or chronicity (acute MCS = 5, VS/UWS = 6; chronic MCS = 21, VS/UWS = 13; average length of time since the injury was 902.3 days, minimum = 2 days, maximum = 9900).

## Group-level connectivity analysis

For the default mode, frontoparietal, salience, auditory, sensorimotor and visual network, functional connectivity encompassed regions classically reported for healthy controls; all six networks showed reduced connectivity in patients in MCS, connectivity was hardly identified in patients in VS/UWS and was absent in comatose patients (Supplementary material).

CRS-R total scores correlated with functional connectivity in key regions of each network (Fig. 2). In contrast, when the CRS-R total scores were used as regressors of connectivity in the cerebellum, which is known for its minimal involvement in consciousness processes (Tononi, 2008), no areas showed connectivity with the behavioural scores. For illustrative purposes, the cerebellar network in healthy controls is presented in the Supplementary material.

The regions that showed higher functional connectivity in patients in MCS compared to VS/UWS for each network are summarized in Fig. 3. To minimize the possibility that differences in functional connectivity reflected differences in brain anatomy, we performed a two-sample *t*-test voxel-based morphometry on the normalized grey matter and white matter segmented masks (smoothed at 6 mm full-width at half-maximum). No differences in grey matter volume between patients in MCS and VS/UWS were identified at FWE  $P < 0.05$  either at the whole-brain or at the cluster-level. Similarly, the analysis of white matter volumes identified no differences between the two groups, even at a liberal threshold  $P < 0.001$  (whole brain level) uncorrected for multiple comparisons. The average grey matter and

white matter volumes in the two patient groups are reported in the Supplementary material.

## Network ranking and selection

All networks were found to discriminate between patients in MCS and VS/UWS with an acceptable accuracy (Supplementary material). Among them, the auditory network was the most highly ranked system to separate patients in MCS from those in VS/UWS.

## Validation with independent data set

Functional connectivity of the auditory network was further used to classify independently assessed patients. The classification was performed on the connectivity strength in bilateral auditory and visual cortices (Fig. 3). This three-feature vector was preferred to a single-feature classification (i.e. the average connectivity across all areas of the auditory network mask) to avoid over-fitting of the classifier. Based on these three clusters' connectivity strength (*z*-values), 20 of 22 patients independently assessed in Salzburg and New York were discriminated congruently (Fig. 4 and Supplementary material), namely the CRS-R diagnosis matched the classification outcome. As in Phillips *et al.* (2011), for each feature we calculated its weighted vector 'w', which determines the orientation of the decision surface, indicative of which feature drives the classification (Bishop, 2006). For the right auditory cortex it was  $w = -1.7890$ , for the left auditory cortex  $w = -0.4002$  and for the occipital cortex  $w = -0.7362$ . The patient who was misclassified as being in MCS had a CRS-R total score of 5 on the day of scanning (indicating the VS/UWS; Patient 11 of centre two, Supplementary material) and she evolved to MCS 38 days later (Auditory Function: 1, Visual Function: 3, Motor Function: 2, Oromotor/Verbal Function: 2, Communication: 0, Arousal: 2). The patient who was misclassified as being in VS/UWS had a CRS-R total score of 9 on the day of scanning (indicating the MCS; Patient 13 of centre two, Supplementary material) based on the presence of localization to noxious stimulation but this behaviour could not be elicited in neither previous (AF: 1, VF: 0, MF: 0, O/VF: 1, COM: 0, AR: 2) or subsequent evaluations (AF: 2, VF: 1, MF: 2, O/VF: 1, COM: 0, AR: 2). To test robustness, we evaluated whether the same classifier generalized to healthy control subjects scanned in Liège and Salzburg ( $n = 39$ ; no healthy control data were available for the New York centre). The majority of healthy controls (37 of 39; 95%) were classified as MCS (Supplementary material).

## Discussion

We here aimed at determining the clinical utility of the resting state functional MRI paradigm in patients with disorders of consciousness by employing a systems-level

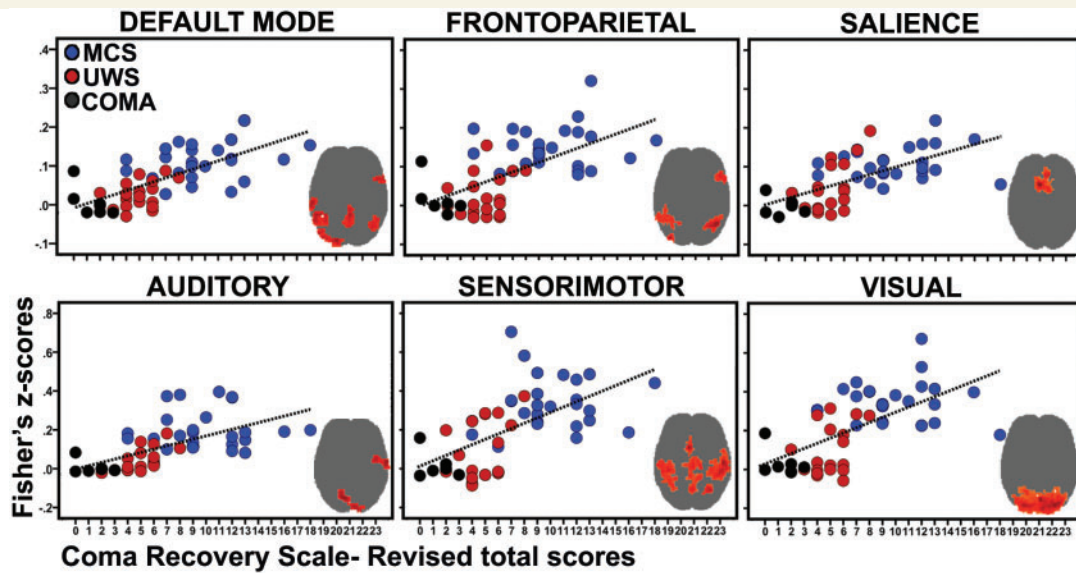


**Figure 2** The intrinsic connectivity networks are involved in consciousness-related processing. Functional connectivity of all studied networks (areas in red) correlate with the level of consciousness as determined by behavioural assessment with the Coma Recovery Scale-Revised (total scores) in patients in MCS, VS/UWS and coma. Statistical maps are thresholded at FWE  $P < 0.05$  (cluster-level) and are rendered on a glass brain template (transverse view).

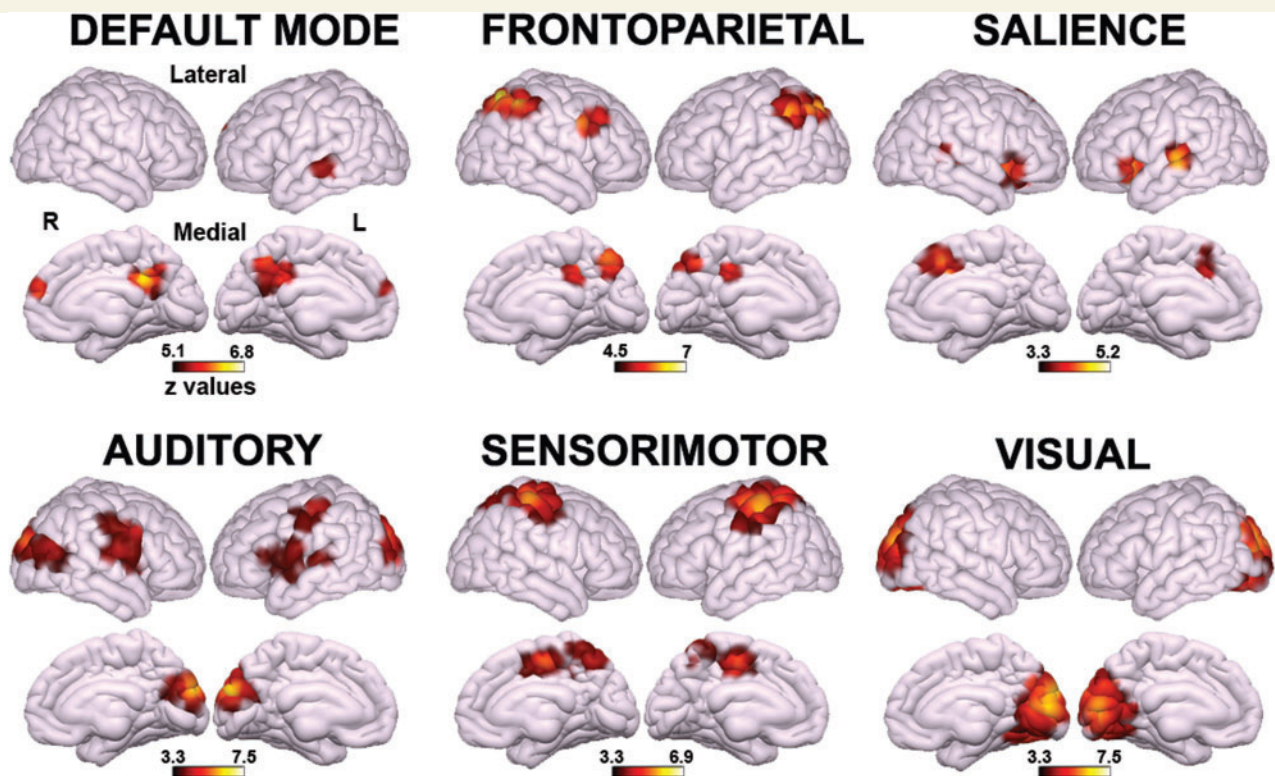


**Figure 3** Regions showing higher functional connectivity in patients in MCS compared to patients in VS/UWS for each network. Statistical maps are thresholded at FWE  $P < 0.05$  (cluster-level) and are rendered on 3D surface plot template (top = lateral view; bottom = medial view).

approach. Resting state functional MRI connectivity of the default mode, frontoparietal, salience, auditory, sensorimotor and visual networks were first shown to correlate with behavioural CRS-R assessment scores, highlighting

their contribution to the level of consciousness. Previous studies on the default mode network, linked to autobiographical memory, mind-wandering, and unconstrained cognition (Buckner *et al.*, 2008), also showed

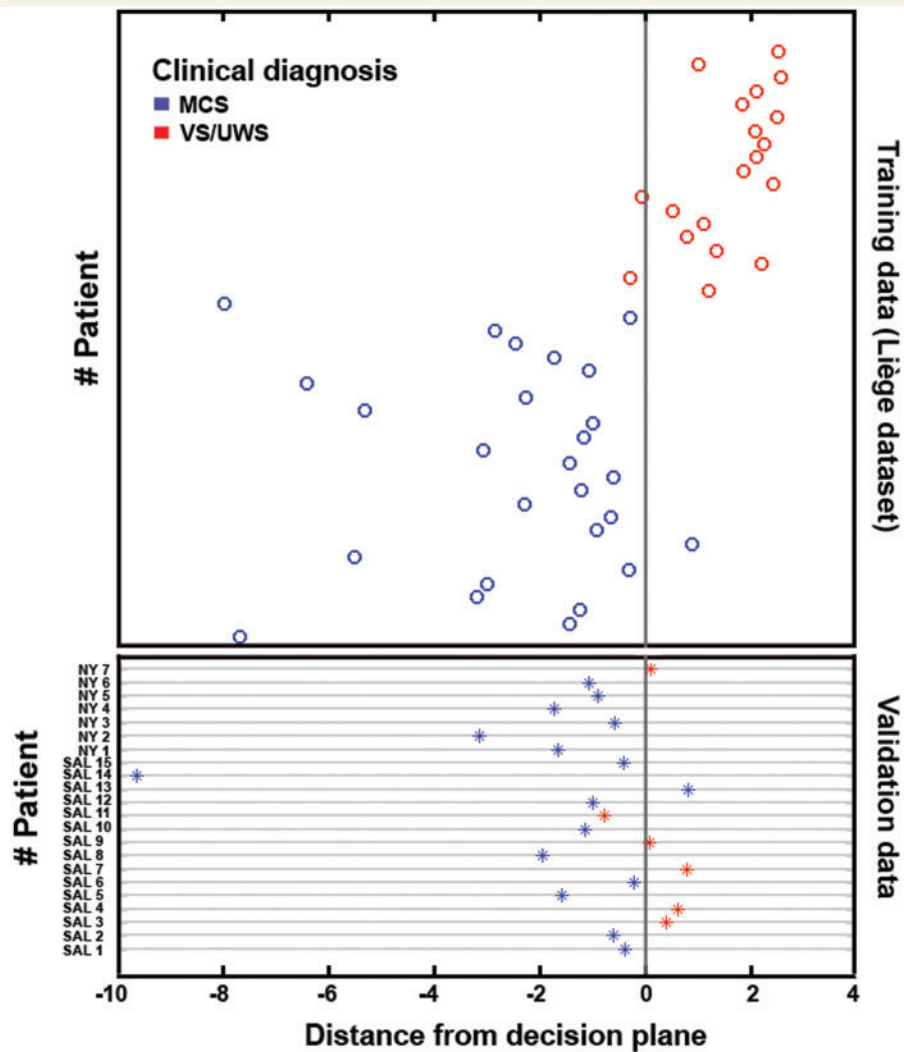


**Figure 4** The auditory-visual crossmodal functional connectivity discriminates single patients in MCS from patients in VS/UWS. The 3D space indicating connectivity between left auditory, right auditory and occipital cortex (Supplementary material) has been compressed into two dimensions to represent the distance of each patient (in circles) from the decision plane (arbitrary values). The *upper* panel plots the data of patients (in circles) who were used for the classifier's training (Liège data set,  $n = 45$ ). The *lower* panel summarizes the classifier's decision on the validation data set including patients (in asterisks) independently assessed in Salzburg ( $n = 15$ ) and New York ( $n = 7$ ). Based on the crossmodal interaction, 20 of the 22 independently assessed patients were classified congruently, namely the behavioural diagnosis matched the classification outcome.

consciousness-level dependent reductions in connectivity under physiological (Horowitz *et al.*, 2009; Samann *et al.*, 2011) and pharmacological unconsciousness (Greicius *et al.*, 2008; Boveroux *et al.*, 2010; Stamatakis *et al.*, 2010; Amico *et al.*, 2014). Similarly, the frontoparietal network, which has been linked to perceptual and somesthetic processing (Smith *et al.*, 2009; Laird *et al.*, 2011) and is considered critical for conscious reportable perception (Dehaene *et al.*, 2003), showed reductions in functional connectivity during sleep (Larson-Prior *et al.*, 2009; Samann *et al.*, 2011; Boly *et al.*, 2012) and anaesthesia (Boveroux *et al.*, 2010). The salience network, which has been involved in conflict monitoring, information integration, response selection, interoceptive processes (Seeley *et al.*, 2007; Smith *et al.*, 2009; Ploner *et al.*, 2010;

Wiech *et al.*, 2010) and the emotional counterpart of pain (Seeley *et al.*, 2007; Shackman *et al.*, 2011), also showed modulations in connectivity under propofol anaesthesia (Guldenmund *et al.*, 2013). Here, the positive correlation between CRS-R scores and the salience network anterior cingulate cortex could account for the preserved capacities of some patients to orient their attentional resources towards environmental salient stimuli, such as noxious stimulation, corroborating previous PET data (Boly *et al.*, 2008). With regards to sensory networks, little changes have been reported under physiological and pharmacological unconsciousness (Heine *et al.*, 2012). Nevertheless, propofol-induced disconnections have been shown between the default mode network and motor cortex, reticular activating system and the thalamus

(Stamatakis *et al.*, 2010). In particular, the thalamus is of critical importance to consciousness (Dehaene and Changeux, 2005; Tononi, 2008). In our analysis the significance of the thalamus was controlled by involving it among the regions of interest in the three large-scale networks, namely the default mode network, frontoparietal and salience. The direct comparison between patients in MCS and VS/UWS did not identify any differences in network-level thalamic connectivity. However, a recent study with patients with disorders of consciousness using a target-detection task showed that respondents had a greater connectivity between the anterior thalamus and prefrontal cortex. These findings suggest that thalamo-frontal circuits are important for cognitive top-down processing (Monti *et al.*, 2015). Interestingly, when the cerebellum was used as a control network, CRS-R total scores did not correlate with any regions of this network in patients. Such findings confirm previous suggestions that the cerebellum has minimal implication in conscious-related processing (Tononi, 2008; Yu *et al.*, 2015). Taken together, the positive correlation between clinical scores and each network's functional connectivity highlight that the here studied networks are an appropriate means to study, at least to a certain degree, residual cognitive function in this patient cohort.

Importantly for clinical practice, we further aimed at determining the capacity of each network to differentiate between patients in MCS and VS/UWS. In terms of functional MRI-based differentiation of patients, to date differences in functional connectivity have been observed only at the group-level for the default mode (Boly *et al.*, 2009; Vanhaudenhuyse *et al.*, 2010; Norton *et al.*, 2012; Soddu *et al.*, 2012; Demertzi *et al.*, 2014), the frontoparietal and the auditory networks (Demertzi *et al.*, 2014). Here, we replicated these findings and further showed group differences in functional connectivity for the salience, sensorimotor and visual networks. Moving towards single-patient network-based differentiation, we found that all networks were able to differentiate patients with an acceptable accuracy (>86%). Such high rate of accuracy can be partly attributed to the fact that the network ranking was based on features extracted from the same population for which between-group differences were already known. To avoid a double-dipping effect, we aimed at validating the most highly ranked network in two independently assessed patient data sets (Salzburg and New York) and across healthy controls. To that end, we opted for single-patient classification based on the connectivity strength of the auditory network. Based on this network's connectivity, 20 of the 22 new patients were classified congruently, i.e. the clinical diagnosis matched the classification outcome. Of note is that the classifier positioned the independently assessed patients closer to the decision plane compared to patients included in the training set. This could be explained by the abovementioned favouring of the Liège training data set during the network ranking procedure, which might have led to a stricter classification of the validation set. Although the intrinsic connectivity networks

have been shown to be robust independent of different scanning parameters (Van Dijk *et al.*, 2010), the different parameters employed in each of the three centres might also have influenced the classifier's estimation. Alternatively, the use of a relevance vector machine classifier (Phillips *et al.*, 2011), which returns probabilities of a patient belonging to a clinical condition instead of using a binary decision, could be a more sensitive way to classify patients less strictly.

The classification results further highlight the challenges posed by behavioural examination (Majerus *et al.*, 2005) which in many cases underestimates patients' level of consciousness (Schnakers *et al.*, 2009). Here, the validation of the auditory network's classifier worked congruently for the majority of the included patients (20/22). Interestingly, the patient who was misclassified as MCS had a profile of VS/UWS on the day of scan but evolved to MCS 38 days later. The other patient was misclassified as VS/UWS but had a clinical profile of MCS on the day of scanning based on the presence of localization to noxious stimulation (note that this behaviour could not be elicited in any other evaluations). The validation of the classifier's outcome to the clinical evaluation was used as a starting point in our analysis. Therefore, a well-defined diagnostic baseline was critical for the subsequent patient classification. To that end, repeated clinical examinations with the CRS-R (average number of assessments  $n = 6$  per patient) were performed. The clinical diagnosis was further confirmed with FDG-PET imaging, which has been shown to have high sensitivity in identifying patients in MCS (Stender *et al.*, 2014). Therefore, patients with an ambiguous profile on clinical assessment and neuroimaging data were not included in the analysis. Similarly, patients who received sedatives to minimize motion in the scanner (Soddu *et al.*, 2011) were further excluded. The reason to exclude sedated patients was because of our limited understanding of the potential effect of anaesthetics on network connectivity (Heine *et al.*, 2012). We here recognize the importance of increasing the classification power for patients scanned after receiving anaesthetics, given that many patients undergo anaesthesia not only to restrict scanner motion but also for neuroprotective reasons (Schifilliti *et al.*, 2010). Future investigations which will aim to disentangle between the variances of anaesthetics and pathology in functional connectivity measures are certainly essential. Finally, even though patients were scanned in an 'awake' state, the monitoring of patients' state of vigilance during data acquisition was not feasible because of technical difficulties. Hence, one cannot exclude the possibility that patients could have fallen asleep during scanning, which could subsequently influence the assessment of functional connectivity.

One explanation of why the auditory network was identified as the system with the highest discriminative capacity could concern its underlying functional neuroanatomy. Apart from temporal cortices, the auditory network further encompasses regions in occipital cortex, pre- and

postcentral areas, insula and anterior cingulate cortex (Damoiseaux *et al.*, 2006; Smith *et al.*, 2009; Laird *et al.*, 2011; Maudoux *et al.*, 2012; Demertzi *et al.*, 2014). The direct comparison between patients in MCS and VS/UWS restricted the identified areas to bilateral auditory and visual cortices. This pattern of auditory-visual functional connectivity has been previously described in normal conscious subjects during rest as well (Eckert *et al.*, 2008) and is in line with functional MRI results in consciousness research. For example, preserved functional MRI activity in temporal and occipital areas has been shown for healthy subjects during mental counting of auditory temporal irregularities; interestingly, this activation was identified only in those subjects who were attentive and aware of the auditory violations (Bekinschtein *et al.*, 2009). At a functional level, the auditory-visual functional connectivity, also referred to as crossmodal interaction, is considered relevant for multisensory integration (Clavagnier *et al.*, 2004). Multisensory integration has been suggested as a facilitator for top-down influences of higher-order regions to create predictions of forthcoming sensory events (Engel *et al.*, 2001). Such top-down connectivity was recently found with an EEG oddball paradigm that differentiated patients in MCS from VS/UWS (Boly *et al.*, 2011). Interestingly, decreased crossmodal auditory-visual interaction has been reported in healthy subjects with preserved structural connections but under pharmacologically-induced anaesthesia (Boveroux *et al.*, 2010). In that study, recovery of consciousness paralleled the restoration of the crossmodal connectivity suggesting a critical role of this connectivity pattern to consciousness level-dependent states.

In our results, the crossmodal interaction was more preserved in patients in MCS compared to unresponsive patients. The reduction in functional connectivity between the auditory-visual cortices in VS/UWS could be partly attributed to disrupted anatomical connections, often encountered in post-comatose patients (Perlberg *et al.*, 2009; Fernandez-Espejo *et al.*, 2010, 2011; Stevens *et al.*, 2014; van der Eerden *et al.*, 2014). The tight link between functional and structural connectivity was recently shown in primates during propofol-induced unconsciousness with regards to resting state functional MRI dynamic fluctuations. In this study, functional connectivity was fluctuating less frequently among distinct consciousness states, it was mostly linked to the state characterizing unconsciousness and this pattern was mostly explained by the underlying structural connectivity (Barttfeld *et al.*, 2015). Here, the negative differences between the two patient groups on voxel-based morphometry of grey and white matter segments is suggestive that the changes in functional connectivity cannot be fully attributed to the underlying anatomical abnormalities. We recognize that analyses with diffusion-weighted imaging and its relation to functional data would allow for more confident statements about residual functional connectivity in our clinical sample.

In conclusion, we here identified that systems-level resting state functional MRI showed consciousness-dependent breakdown not only for the default mode network but also for the frontoparietal, salience, auditory, sensorimotor and visual networks. Functional connectivity between auditory and visual cortices was the most sensitive feature to accurately discriminate single patients into the categories of MCS and VS/UWS. Our findings point to the significance of multisensory integration and top-down processes in consciousness seemingly supported by crossmodal connectivity. In the future, efforts need to be made to promote the feasibility of such a complex approach in the clinical setting and promote the clinical utility of the resting paradigm for single-patient diagnostics.

## Acknowledgements

We would like to thank Lionel Naccache and Jacobo Sitt for useful suggestions on the manuscript preparation and data illustration, and Xiaoqian Jenny Chai for code sharing.

## Funding

A.D. is postdoctoral Researcher at the Belgian National Funds for Scientific Research (FNRS), L.H. and V.C.V. are Research Fellows at the FNRS, S.L. is Research Director at the FNRS. This work was further supported by the European Commission, the James McDonnell Foundation, the European Space Agency, Mind Science Foundation, the French Speaking Community Concerted Research Action (ARC - 06/11 - 340), the Public Utility Foundation 'Université Européenne du Travail', 'Fondazione Europea di Ricerca Biomedica' and the University and University Hospital of Liège.

## Supplementary material

Supplementary material is available at *Brain* online.

## References

- Achard S, Delon-Martin C, Vertes PE, Renard F, Schenck M, Schneider F, et al. Hubs of brain functional networks are radically reorganized in comatose patients. *Proc Natl Acad Sci USA* 2012; 109: 20608–13.
- Achard S, Kremer S, Schenck M, Renard F, Ong-Nicolas C, Namer JJ, et al. Global functional disconnections in post-anoxic coma patient. *Neuroradiol J* 2011; 24: 311–5.
- Amico E, Gomez F, Di Perri C, Vanhauzenhuyse A, Lesenfants D, Boveroux P, et al. Posterior cingulate cortex-related co-activation patterns: a resting state fMRI study in propofol-induced loss of consciousness. *PLoS One* 2014; 9: e100012.
- Bardin JC, Schiff ND, Voss HU. Pattern classification of volitional functional magnetic resonance imaging responses in patients with severe brain injury. *Arch Neurol* 2012; 69: 176–81.

- Bartfeld P, Uhrig L, Sitt JD, Sigman M, Jarraya B, Dehaene S. Signature of consciousness in the dynamics of resting-state brain activity. *Proc Natl Acad Sci USA* 2015; 112: 887–92.
- Behzadi Y, Restom K, Liu J, Liu TT. A component based noise correction method (CompCor) for BOLD and perfusion based fMRI. *Neuroimage* 2007; 37: 90–101.
- Bekinschtein TA, Dehaene S, Rohaut B, Tadel F, Cohen L, Naccache L. Neural signature of the conscious processing of auditory regularities. *Proc Natl Acad Sci USA* 2009; 106: 1672–7.
- Bishop CM. (2006). *Pattern Recognition and Machine Learning*. Singapore: Springer.
- Boly M, Faymonville M-E, Schnakers C, Peigneux P, Lambermont B, Phillips C, et al. Perception of pain in the minimally conscious state with PET activation: an observational study. *Lancet Neurol* 2008; 7: 1013–20.
- Boly M, Garrido MI, Gosseries O, Bruno MA, Boveroux P, Schnakers C, et al. Preserved feedforward but impaired top-down processes in the vegetative state. *Science* 2011; 332: 858–62.
- Boly M, Perlberg V, Marrelec G, Schabus M, Laureys S, Doyon J, et al. Hierarchical clustering of brain activity during human nonrapid eye movement sleep. *Proc Natl Acad Sci USA* 2012; 109: 5856–61.
- Boly M, Tshibanda L, Vanhaudenhuyse A, Noirhomme Q, Schnakers C, Ledoux D, et al. Functional connectivity in the default network during resting state is preserved in a vegetative but not in a brain dead patient. *Hum Brain Mapp* 2009; 30: 2393–400.
- Boveroux P, Vanhaudenhuyse A, Bruno MA, Noirhomme Q, Lauwick S, Luxen A, et al. Breakdown of within- and between-network resting state functional magnetic resonance imaging connectivity during propofol-induced loss of consciousness. *Anesthesiology* 2010; 113: 1038–53.
- Bruno MA, Soddu A, Demertzi A, Laureys S, Gosseries O, Schnakers C, et al. Disorders of consciousness: moving from passive to resting state and active paradigms. *Cog Neurosci* 2010; 1: 193–203.
- Buckner RL, Andrews-Hanna JR, Schacter DL. The brain's default network: anatomy, function, and relevance to disease. *Ann N Y Acad Sci* 2008; 1124: 1–38.
- Burges C. A tutorial on support vector machines for pattern recognition. *Data Min Knowl Discov* 1998; 2: 121–67.
- Casali AG, Gosseries O, Rosanova M, Boly M, Sarasso S, Casali KR, et al. A theoretically based index of consciousness independent of sensory processing and behavior. *Sci Transl Med* 2013; 5: 198ra05.
- Chai XJ, Castanon AN, Ongur D, Whitfield-Gabrieli S. Anticorrelations in resting state networks without global signal regression. *Neuroimage* 2012; 59: 1420–8.
- Clavagnier S, Falchier A, Kennedy H. Long-distance feedback projections to area V1: implications for multisensory integration, spatial awareness, and visual consciousness. *Cogn Affect Behav Neurosci* 2004; 4: 117–26.
- Cole DM, Smith SM, Beckmann CF. Advances and pitfalls in the analysis and interpretation of resting-state FMRI data. *Front Syst Neurosci* 2010; 4: 8.
- Coleman MR, Rodd JM, Davis MH, Johnsrude IS, Menon DK, Pickard JD, et al. Do vegetative patients retain aspects of language comprehension? Evidence from fMRI. *Brain* 2007; 130: 2494–507.
- Crone JS, Soddu A, Holler Y, Vanhaudenhuyse A, Schurz M, Bergmann J, et al. Altered network properties of the fronto-parietal network and the thalamus in impaired consciousness. *Neuroimage Clin* 2014; 4: 240–48.
- Damoiseaux JS, Rombouts SA, Barkhof F, Scheltens P, Stam CJ, Smith SM, et al. Consistent resting-state networks across healthy subjects. *Proc Natl Acad Sci USA* 2006; 103: 13848–53.
- De Martino F, Gentile F, Esposito F, Balsi M, Di Salle F, Goebel R, et al. Classification of fMRI independent components using IC-fingerprints and support vector machine classifiers. *Neuroimage* 2007; 34: 177–94.
- Dehaene S, Changeux JP. Ongoing spontaneous activity controls access to consciousness: a neuronal model for inattentive blindness. *PLoS Biol* 2005; 3: e141.
- Dehaene S, Sergent C, Changeux JP. A neuronal network model linking subjective reports and objective physiological data during conscious perception. *Proc Natl Acad Sci USA* 2003; 100: 8520–5.
- Demertzi A, Gómez F, Crone JS, Vanhaudenhuyse A, Tshibanda L, Noirhomme Q, et al. Multiple fMRI system-level baseline connectivity is disrupted in patients with consciousness alterations. *Cortex* 2014; 52: 35–46.
- Di HB, Yu SM, Weng XC, Laureys S, Yu D, Li JQ, et al. Cerebral response to patient's own name in the vegetative and minimally conscious states. *Neurology* 2007; 68: 895–9.
- Eckert MA, Kamdar NV, Chang CE, Beckmann CF, Greicius MD, Menon V. A cross-modal system linking primary auditory and visual cortices: evidence from intrinsic fMRI connectivity analysis. *Hum Brain Mapp* 2008; 29: 848–57.
- Edlow BL, Giacino JT, Wu O. Functional MRI and outcome in traumatic coma. *Curr Neurol Neurosci Rep* 2013; 13: 1–11.
- Engel AK, Fries P, Singer W. Dynamic predictions: oscillations and synchrony in top-down processing. *Nat Rev Neurosci* 2001; 2: 704–16.
- Fernandez-Espejo D, Bekinschtein T, Monti MM, Pickard JD, Junque C, Coleman MR, et al. Diffusion weighted imaging distinguishes the vegetative state from the minimally conscious state. *Neuroimage* 2011; 54: 103–12.
- Fernandez-Espejo D, Junque C, Cruse D, Bernabeu M, Roig-Rovira T, Fabregas N, et al. Combination of diffusion tensor and functional magnetic resonance imaging during recovery from the vegetative state. *BMC Neurol* 2010; 10: 77.
- Fox MD, Snyder AZ, Vincent JL, Corbetta M, Van Essen DC, Raichle ME. The human brain is intrinsically organized into dynamic, anticorrelated functional networks. *Proc Natl Acad Sci USA* 2005; 102: 9673–8.
- Giacino JT, Ashwal S, Childs N, Cranford R, Jennett B, Katz DI, et al. The minimally conscious state: Definition and diagnostic criteria. *Neurology* 2002; 58: 349–53.
- Giacino JT, Fins JJ, Laureys S, Schiff ND. Disorders of consciousness after acquired brain injury: the state of the science. *Nat Rev Neurol* 2014; 10: 99–114.
- Giacino JT, Kalmar K, Whyte J. The JFK Coma Recovery Scale-Revised: measurement characteristics and diagnostic utility. *Arch Phys Med Rehabil* 2004; 85: 2020–9.
- Greicius MD, Kiviniemi V, Tervonen O, Vainionpää V, Alahuhta S, Reiss AL, et al. Persistent default-mode network connectivity during light sedation. *Hum Brain Mapp* 2008; 29: 839–47.
- Greicius MD, Krasnow B, Reiss AL, Menon V. Functional connectivity in the resting brain: a network analysis of the default mode hypothesis. *Proc Natl Acad Sci USA* 2003; 100: 253–8.
- Guldenmund P, Demertzi A, Boveroux P, Boly M, Vanhaudenhuyse A, Bruno MA, et al. Thalamus, brainstem and salience network connectivity changes during propofol-induced sedation and unconsciousness. *Brain Connect* 2013; 3: 273–85.
- Heine L, Soddu A, Gomez F, Vanhaudenhuyse A, Tshibanda L, Thonnard M, et al. Resting state networks and consciousness. Alterations of multiple resting state network connectivity in physiological, pharmacological and pathological consciousness states. *Front Psychol* 2012; 3: 1–12.
- Horowitz SG, Braun AR, Carr WS, Picchioni D, Balkin TJ, Fukunaga M, et al. Decoupling of the brain's default mode network during deep sleep. *Proc Natl Acad Sci USA* 2009; 106: 11376–81.
- Huang Z, Dai R, Wu X, Yang Z, Liu D, Hu J, et al. The self and its resting state in consciousness: an investigation of the vegetative state. *Hum Brain Mapp* 2014; 35: 1997–2008.
- Jennett B, Plum F. Persistent vegetative state after brain damage. A syndrome in search of a name. *Lancet* 1972; 1: 734–7.
- Kelly RE Jr, Alexopoulos GS, Wang Z, Gunning FM, Murphy CF, Morimoto SS, et al. Visual inspection of independent components:

- defining a procedure for artifact removal from fMRI data. *J Neurosci Methods* 2010; 189: 233–45.
- Laird AR, Fox PM, Eickhoff SB, Turner JA, Ray KL, McKay DR, et al. Behavioral interpretations of intrinsic connectivity networks. *J Cogn Neurosci* 2011; 23: 4022–37.
- Larson-Prior LJ, Zempel JM, Nolan TS, Prior FW, Snyder AZ, Raichle ME. Cortical network functional connectivity in the descent to sleep. *Proc Natl Acad Sci USA* 2009; 106: 4489–94.
- Laureys S, Celesia G, Cohadon F, Lavrijsen J, Leon-Carrion J, Sannita WG, et al. Unresponsive wakefulness syndrome: a new name for the vegetative state or apallic syndrome. *BMC Med* 2010; 8: 68.
- Majerus S, Gill-Thwaites H, Andrews K, Laureys S. Behavioral evaluation of consciousness in severe brain damage. *Prog Brain Res* 2005; 150: 397–413.
- Maki-Marttunen V, Diez I, Cortes JM, Chialvo DR, Villarreal M. Disruption of transfer entropy and inter-hemispheric brain functional connectivity in patients with disorder of consciousness. *Front Neuroinform* 2013; 7: 24.
- Maudoux A, Lefebvre P, Cabay JE, Demertzi A, Vanhaudenhuyse A, Laureys S, et al. Auditory resting-state network connectivity in tinnitus: a functional MRI study. *PLoS One* 2012; 7: e36222.
- Monti MM, Rosenberg M, Finoia P, Kamau E, Pickard JD, Owen AM. Thalamo-frontal connectivity mediates top-down cognitive functions in disorders of consciousness. *Neurology* 2015; 84: 167–73.
- Monti MM, Vanhaudenhuyse A, Coleman MR, Boly M, Pickard JD, Tshibanda L, et al. Willful modulation of brain activity in disorders of consciousness. *N Engl J Med* 2010; 362: 579–89.
- Murphy K, Birn RM, Handwerker DA, Jones TB, Bandettini PA. The impact of global signal regression on resting state correlations: are anti-correlated networks introduced? *Neuroimage* 2009; 44: 893–905.
- Norton L, Hutchison RM, Young GB, Lee DH, Sharpe MD, Mirsattari SM. Disruptions of functional connectivity in the default mode network of comatose patients. *Neurology* 2012; 78: 175–81.
- Ovadia-Caro S, Nir Y, Soddu A, Ramot M, Hesselmann G, Vanhaudenhuyse A, et al. Reduction in inter-hemispheric connectivity in disorders of consciousness. *PLoS One* 2012; 7: e37238.
- Owen AM, Coleman MR, Boly M, Davis MH, Laureys S, Pickard JD. Detecting awareness in the vegetative state. *Science* 2006; 313: 1402.
- Perlberg V, Puybasset L, Tollard E, Lehericy S, Benali H, Galanaud D. Relation between brain lesion location and clinical outcome in patients with severe traumatic brain injury: a diffusion tensor imaging study using voxel-based approaches. *Hum Brain Mapp* 2009; 30: 3924–33.
- Phillips CL, Bruno MA, Maquet P, Boly M, Noirhomme Q, Schnakers C, et al. “Relevance vector machine” consciousness classifier applied to cerebral metabolism of vegetative and locked-in patients. *Neuroimage* 2011; 56: 797–808.
- Ploner M, Lee MC, Wiech K, Bingel U, Tracey I. Prestimulus functional connectivity determines pain perception in humans. *Proc Natl Acad Sci USA* 2010; 107: 355–60.
- Raichle ME, MacLeod AM, Snyder AZ, Powers WJ, Gusnard DA, Shulman GL. A default mode of brain function. *Proc Natl Acad Sci USA* 2001; 98: 676–82.
- Rosanov M, Gosseries O, Casarotto S, Boly M, Casali AG, Bruno MA, et al. Recovery of cortical effective connectivity and recovery of consciousness in vegetative patients. *Brain* 2012; 135: 1308–20.
- Saad ZS, Gotts SJ, Murphy K, Chen G, Jo HJ, Martin A, et al. Trouble at rest: how correlation patterns and group differences become distorted after global signal regression. *Brain Connect* 2012; 2: 25–32.
- Saeyes Y, Inza I, Larranaga P. A review of feature selection techniques in bioinformatics. *Bioinformatics* 2007; 23: 2507–17.
- Samann PG, Wehrle R, Hoehn D, Spormaker VI, Peters H, Tully C, et al. Development of the brain’s default mode network from wakefulness to slow wave sleep. *Cereb Cortex* 2011; 21: 2082–93.
- Sanders RD, Tononi G, Laureys S, Sleigh JW. Unresponsiveness not equal unconsciousness. *Anesthesiology* 2012; 116: 946–59.
- Schiff ND, Rodriguez-Moreno D, Kamal A, Kim KH, Giacino JT, Plum F, et al. fMRI reveals large-scale network activation in minimally conscious patients. *Neurology* 2005; 64: 514–23.
- Schiffli D, Grasso G, Conti A, Fodale V. Anaesthetic-related neuroprotection: intravenous or inhalational agents? *CNS Drugs* 2010; 24: 893–907.
- Schnakers C, Vanhaudenhuyse A, Giacino JT, Ventura M, Boly M, Majerus S, et al. Diagnostic accuracy of the vegetative and minimally conscious state: clinical consensus versus standardized neurobehavioral assessment. *BMC Neurol* 2009; 9: 35.
- Seeley WW, Menon V, Schatzberg AF, Keller J, Glover GH, Kenna H, et al. Dissociable intrinsic connectivity networks for salience processing and executive control. *J Neurosci* 2007; 27: 2349–56.
- Shackman AJ, Salomons TV, Slagter HA, Fox AS, Winter JJ, Davidson RJ. The integration of negative affect, pain and cognitive control in the cingulate cortex. *Nat Rev Neurosci* 2011; 12: 154–67.
- Sitt JD, King JR, El Karoui I, Rohaut B, Faugeras F, Gramfort A, et al. Large scale screening of neural signatures of consciousness in patients in a vegetative or minimally conscious state. *Brain* 2014; 137: 2258–70.
- Smith SM, Fox PT, Miller KL, Glahn DC, Fox PM, Mackay CE, et al. Correspondence of the brain’s functional architecture during activation and rest. *Proc Natl Acad Sci USA* 2009; 106: 13040–5.
- Soddu A, Vanhaudenhuyse A, Bahri MA, Bruno MA, Boly M, Demertzi A, et al. Identifying the default-mode component in spatial IC analyses of patients with disorders of consciousness. *Hum Brain Mapp* 2012; 33: 778–96.
- Soddu A, Vanhaudenhuyse A, Demertzi A, Bruno MA, Tshibanda L, Di H, et al. Resting state activity in patients with disorders of consciousness. *Funct Neurol* 2011; 26: 37–43.
- Stamatakis EA, Adapa RM, Absalom AR, Menon DK. Changes in resting neural connectivity during propofol sedation. *PLoS One* 2010; 5: e14224.
- Stender J, Gosseries O, Bruno MA, Charland-Verville V, Vanhaudenhuyse A, Demertzi A, et al. Diagnostic precision of PET imaging and functional MRI in disorders of consciousness: a clinical validation study. *Lancet* 2014; 384: 514–22.
- Stevens RD, Hannawi Y, Puybasset L. MRI for coma emergence and recovery. *Curr Opin Crit Care* 2014; 20: 168–73.
- Tononi G. Consciousness as integrated information: a provisional manifesto. *Biol Bull* 2008; 215: 216–42.
- Tsai YH, Yuan R, Huang YC, Yeh MY, Lin CP, Biswal BB. Disruption of brain connectivity in acute stroke patients with early impairment in consciousness. *Front Psychol* 2014; 4: 956.
- van der Eerden AW, Khalilzadeh O, Perlberg V, Dinkel J, Sanchez P, Vos PE, et al. White matter changes in comatose survivors of anoxic ischemic encephalopathy and traumatic brain injury: comparative diffusion-tensor imaging study. *Radiology* 2014; 270: 506–16.
- Van Dijk KR, Hedden T, Venkataraman A, Evans KC, Lazar SW, Buckner RL. Intrinsic functional connectivity as a tool for human connectomics: theory, properties, and optimization. *J Neurophysiol* 2010; 103: 297–321.
- Van Dijk KR, Sabuncu MR, Buckner RL. The influence of head motion on intrinsic functional connectivity MRI. *Neuroimage* 2012; 59: 431–38.
- Vanhaudenhuyse A, Demertzi A, Schabus M, Noirhomme Q, Bredart S, Boly M, et al. Two distinct neuronal networks mediate the awareness of environment and of self. *J Cogn Neurosci* 2011; 23: 570–8.
- Vanhaudenhuyse A, Noirhomme Q, Tshibanda LJ, Bruno MA, Boveroux P, Schnakers C, et al. Default network connectivity reflects the level of consciousness in non-communicative brain-damaged patients. *Brain* 2010; 133: 161–71.

- Whitfield-Gabrieli S, Nieto-Castanon A. Conn: a functional connectivity toolbox for correlated and anticorrelated brain networks. *Brain Connect* 2012; 2: 125–41.
- Wiech K, Lin CS, Brodersen KH, Bingel U, Ploner M, Tracey I. Anterior insula integrates information about salience into perceptual decisions about pain. *J Neurosci* 2010; 30: 16324–31.
- Wong CW, Olafsson V, Tal O, Liu TT. Anti-correlated networks, global signal regression, and the effects of caffeine in resting-state functional MRI. *Neuroimage* 2012; 63: 356–64.
- Yu F, Jiang QJ, Sun XY, Zhang RW. A new case of complete primary cerebellar agenesis: clinical and imaging findings in a living patient. *Brain* 2015; 138: e353.